Infrared switching from resonant to passive photonic bandgaps: transition from purely photonic to hybrid electronic/photonic systems

2009 J. Phys.: Condens. Matter 21 155801

(http://iopscience.iop.org/0953-8984/21/15/155801)

IOP Publishing Journal of Physics: Condensed Matter

J. Phys.: Condens. Matter **21** (2009) 155801 (7pp) doi:10.1088/0953-8984/21/15/155801

Infrared switching from resonant to passive photonic bandgaps: transition from purely photonic to hybrid electronic/photonic systems

S M Sadeghi[1] **and W Li**[2]

[1] Department of Physics, University of Alabama in Huntsville, Huntsville, AL 35899, USA
[2] Department of Chemistry and Engineering Physics, University of Wisconsin-Platteville, Platteville, WI 53818, USA

E-mail: seyed.sadeghi@uah.edu

Received 28 November 2008, in final form 19 February 2009
Published 17 March 2009
Online at stacks.iop.org/JPhysCM/21/155801

Abstract

Coherently controlled optical processes have been extensively studied in various systems including atoms, quantum wells and quantum dots. In this study we investigate such processes in Bragg multi-quantum well resonant (active) photonic bandgaps, wherein the dipole–dipole interwell interaction couples different quantum wells together, forming supperradiant exciton modes. Our results show that in such systems one can use an infrared laser beam to replace the collective superradiant mode with an electromagnetically induced transparency mode, demonstrating infrared switching of an active photonic bandgap to a hybrid system. Such a hybrid system consists of a passive photonic bandgap and an electromagnetically induced transparency band window superimposed on each other. A detailed study of the interplay between the collective and infrared-induced exciton excitations of quantum wells in Bragg multi-quantum well resonant photonic bandgap structures is presented.

(Some figures in this article are in colour only in the electronic version)

1. Introduction

Excitons in multi-quantum well (MQW) structures can be strongly coupled together via dipole–dipole interaction that is mediated by re-emitted photons and light propagation in such structures [1, 2]. The resulting interwell coupling then causes collective excitation of these structures, leading to significant modifications of their optical responses. In particular, when the interwell separation between the QWs is an integer multiple of the half optical wavelength, the MQW structure becomes a Bragg structure, wherein the oscillator strengths of all oscillators are concentrated in one superradiant mode [3]. Under this condition the radiative linewidth of the MQW structure becomes very broad, forming an active photonic bandgap (PBG).

In a recent paper we studied coherent control of Bragg MQW structures using infrared (IR) dressing of excitons [4]. To do this, as shown schematically in figure 1, we considered a QW structure such that it contained two conduction subbands. Therefore, in the presence of an IR field polarized along the growth direction (z) these two subbands could be coherently coupled to each other. The superradiant mode in such a structure, like any other active MQW PBGs, was associated with the excitons correlated with the first conduction (e1) and valence (hh1) subbands (the e1–hh1 excitons). As a result, in the absence of the IR field this structure exhibited similar active PBGs [2, 3]. In the presence of the IR laser field (control field), however, such excitons were strongly mixed with the excitons associated with the second conduction subband (e2) and hh1 (e2–hh1). We showed that such a dressing process could dramatically change the collective response of the MQW. This included formation of photonic electromagnetically induced transparency (P-EIT). In such a process a transparency window is driven within the active PBG in the vicinity of the Bragg wavelength, making the structure transparent around this wavelength.

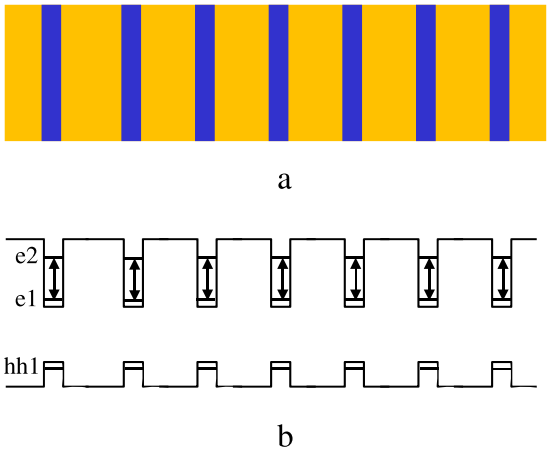

Figure 1. Schematic diagram of the Bragg MQW structure interacting with an intense IR laser field. e1 and e2 refer to the conduction subbands and hh1 represent the heavy-hole subband. The two-sided arrows refer to the mixing processes caused by the IR laser.

A unique feature of IR dressing of MQW structures, such as that shown in figure 1, is the amount of control it provides to us to adjust contributions of two governing features in Bragg MQW PBG structures. These two features are the superradiant mode of excitons and the background refractive index contrast between the wells and barriers. When the dressing effects are insignificant or the IR field is off the superradiant mode is the dominant mode of the PBG structure. Under this condition these two features are strongly entangled together. When the IR dressing of the QWs is significant the superradiant mode collapses. Under this condition, effects associated with the excitons and those associated with the background refractive index contrast of the wells and barriers are completely disentangled from each other.

Our objective in this paper is to utilize these features to study coherent control of the optical responses of Bragg MQW active PBG structures. This will be done by adjusting the balance between the interwell coupling of the QWs (superradiant mode contribution) and infrared coupling of the QWs (optical coherent contributions). In particular, we will study the case where the supperradiant mode is replaced by an electromagnetically induced transparency (EIT) mode. Under this condition we will have a hybridized photonic/electronic system that includes a passive PBG formed by the background refractive index contrast of the wells and barriers (off-resonant contribution) and a coherently generated electronic transmission bandgap or band splitting associated with the EIT of excitons. We show that these two independent contributions are superimposed on each other, forming a central peak, which is immune against the infrared laser, in the middle of the transparency window of the EIT.

Note that EIT is a process happening when the upper level of a transition is coupled via a laser field to another level, reducing absorption of the transition significantly [5]. This process has been extensively studied in atoms and solids, including QWs and quantum dots [6]. EIT in the intersubband transitions of n-doped QWs has also been used to develop active (resonant) PBG and to design optical devices such as distributed feedback lasers [7]. Additionally, the effects of PBG on EIT have been studied considering the electronic transitions near or within the photonic bandgap [8]. It has also been shown that, when a resonantly absorbing medium, which can support EIT, is imposed on a standing wave of an optical field, it can generate a fully developed PBG [9].

MQW-active PBG structures have already been studied for their numerous applications. These include polariton amplification, all-optical switching [10, 11], optical delay lines [12], and stopping, storing and releasing light pulses [13, 14]. The results of this paper illustrate new functionalities of such structures via coherent control of their optical processes. Therefore, they will lead to new applications and enhancement of the previously studied ones. On the other hand, since one of the signatures of the coherently controlled optical processes discussed in this paper is the combination of two types of optical coupling processes, i.e. collective interwell coupling (spatial coupling) and optical coupling (localized coupling), these results can be of particular interest for investigation of a diversified class of coherently controlled optical processes in solids.

2. Multi-subband mixing of excitons in Bragg multi-quantum well structures

Excitonic transitions (resonant effects) and background refractive index perturbation associated with the wells and barriers (off-resonant effects) are the two main features determining the reflection and transmission of MQW-active PBGs. To study how an IR laser field can manipulate contributions of these features and coherently control the bandgaps, we consider a probe field that is propagating along the growth direction (z) of the structure shown in figure 1. This structure also interacts with an IR field (control field) with polarization along z. We consider each period of this structure consists of a GaAs/$Al_{0.2}Ga_{0.8}As$ QW supporting two conduction subbands, e1 and e2.

Since here we are only interested in the linear response of the system, propagation of the probe field along z can be described by [15, 16]

$$\left[\frac{\mathrm{d}^2}{\mathrm{d}z^2}+\left(\frac{\omega_\mathrm{s}}{c}\right)^2\varepsilon_0(z)\right]E^{\omega_\mathrm{c},I_\mathrm{c}}(z)=-\left(\frac{\omega_\mathrm{s}}{c}\right)^2 4\pi P_\mathrm{exc}^{\omega_\mathrm{c},I_\mathrm{c}}(z). \tag{1}$$

Here $\varepsilon_0 = n_\mathrm{b}^2$ or n_w^2 and ω_s represents the interband probe or signal frequency. n_b and n_w are the background refractive indices of the barriers and wells, respectively. $P_\mathrm{exc}^{\omega_\mathrm{c},I_\mathrm{c}}$ is related to the exciton susceptibility, $\chi_\mathrm{exc}^{\omega_\mathrm{c},I_\mathrm{c}}(\omega_\mathrm{s})$, for given values of the control field intensity (I_c) and frequency (ω_c) according to

$$P_\mathrm{exc}^{\omega_\mathrm{c},I_\mathrm{c}}=\chi_\mathrm{exc}^{\omega_\mathrm{c},I_\mathrm{c}}(\omega_\mathrm{s})\varepsilon_0\int\Phi_\mathrm{1s}^\mathrm{exc}(z)\Phi_\mathrm{1s}^\mathrm{exc}(z')E^{\omega_\mathrm{c},I_\mathrm{c}}(z')\,\mathrm{d}z'. \tag{2}$$

Here $\Phi_\mathrm{1s}^\mathrm{exc}(z)$ refer to the envelope functions of the 1s states of the e1–hh1 excitons.

$\chi_\mathrm{exc}^{\omega_\mathrm{c},I_\mathrm{c}}(\omega_\mathrm{s})$ is the main agent for transferring the coherent effects to the MQW structure. To see this, first let us consider

the Hamiltonian of the QW structure in the presence of the IR field:

$$H = H_0 + V + H_{\rm int}. \tag{3}$$

H_0 contains the single-particle energies of electrons and holes, and is given by

$$H_0 = \sum_{n_{\rm c},\mathbf{k}} E^{\rm c}(n_{\rm c},\mathbf{k}) a^{\dagger}_{n_{\rm c},\mathbf{k}} a_{n_{\rm c},\mathbf{k}} + \sum_{n_{\rm v},\mathbf{k}} E^{\rm v}(n_{\rm v},\mathbf{k}) a^{\dagger}_{n_{\rm v},\mathbf{k}} a_{n_{\rm v},\mathbf{k}}. \tag{4}$$

$E^{\rm c}(n_{\rm c},\mathbf{k})$ and $E^{\rm v}(n_{\rm v},\mathbf{k})$ are the electron energies for states $|n_{\rm c},\mathbf{k}\rangle$ and $|n_{\rm v},\mathbf{k}\rangle$ in the conduction and valence subbands labeled by $n_{\rm c}$ and $n_{\rm v}$. For the special case studied in this paper we only consider the first heavy-hole valence band (v = hh1) and the first two conduction subbands, i.e. $n_{\rm c}$ = e1 and e2. $\mathbf{k}$ is the electron wavevector in the plane of the QW. Parabolic dispersion relations are used to describe the in-plane kinetics, where the effective masses are taken to be independent of the subband indices. $a^{\dagger}_{n_{\rm c},\mathbf{k}}$ and $a_{n_{\rm c},\mathbf{k}}$ are the creation and annihilation operators for electrons in the conduction subband with index $n_{\rm c}$, and $a^{\dagger}_{n_{\rm v},\mathbf{k}}$ and $a_{n_{\rm v},\mathbf{k}}$ are the corresponding operators for electrons in the valence subbands. We treat the case of low interband excitation, in which electron–electron and hole–hole interactions may be neglected. Coulomb mixing between different subbands is considered negligible since we focus on QWs with well width <15 nm [17]. With these considerations, the Coulomb operator in equation (3), which describes electron–hole interactions, is of the form

$$V = \sum_{n_{\rm c},n_{\rm v}} \sum_{\mathbf{k},\mathbf{k}',\mathbf{q}\neq 0} V_{n_{\rm c},n_{\rm v}}(\mathbf{q}) a^{\dagger}_{n_{\rm c},\mathbf{k}+\mathbf{q}} a^{\dagger}_{n_{\rm v},\mathbf{k}'-\mathbf{q}} a_{n_{\rm v},\mathbf{k}'} a_{n_{\rm c},\mathbf{k}}, \tag{5}$$

where $V_{n_{\rm c},n_{\rm v}}(\mathbf{q})$ is the matrix element of the Coulomb operator between the single-particle states and $\mathbf{q}$ is the wavevector exchanged in the particle interaction.

The IR field laser field ($E(t) = E{\rm e}^{-{\rm i}\omega_{\rm c}t}$) has a frequency ($\omega_{\rm c}$) which is near resonant with the $|{\rm e1},\mathbf{k}\rangle$ to $|{\rm e2},\mathbf{k}\rangle$ (e1–e2) transition. Therefore, within the electric-dipole and rotating wave approximations, the interaction term is given by

$$H_{\rm int} = \hbar \sum_{\mathbf{k}} \{\mu_{12} E(t) a^{\dagger}_{{\rm e2},\mathbf{k}} a_{{\rm e1},\mathbf{k}} + \mu^{*}_{12} E^{*}(t) a^{\dagger}_{{\rm e1},\mathbf{k}} a_{{\rm e2},\mathbf{k}}\}. \tag{6}$$

Here μ_{12} is the z component of the matrix element of the electric-dipole operator between single-electron states in the conduction subbands.

Given the total Hamiltonian in equation (3), one may obtain the equations of motion for the system's density matrix:

$$\frac{\partial \rho^{\mathbf{k}}}{\partial t} = -\frac{\rm i}{\hbar}[H,\rho^{\mathbf{k}}] + \left.\frac{\partial \rho^{\mathbf{k}}}{\partial t}\right|_{\rm relax}. \tag{7}$$

The second term in this equation represents the corresponding damping terms. The optical Bloch equations can then be transformed into an excitonic basis, acquiring the following form [18]:

$$\frac{{\rm d}\mathbf{\Lambda}^{ij,\beta}}{{\rm d}t} = \mathbf{L}^{ij,\beta}\mathbf{\Lambda}^{ij,\beta} + \mathbf{K}^{ij,\beta}. \tag{8}$$

Here the matrix $\mathbf{\Lambda}^{ij,\beta}$ contains the density matrix elements in the excitonic basis (i = e1 and j = hh1), while $\mathbf{L}^{ij,\beta}$ and $\mathbf{K}^{ij,\beta}$ consist of their coefficients, and β is the energy index.

To calculate the interband susceptibility associated with the e1–hh1 excitons, we employ linear response theory. For β = 1s we have

$$\chi^{\omega_{\rm c},I_{\rm c}}_{\rm exc}(\omega_{\rm s}) = \hat{A}\langle[P^{+}_{\rm 1s}(t'), \tilde{P}^{-}_{\rm 1s}(t',z_1)]\rangle|_{z_1={\rm i}\omega_{\rm s}}. \tag{9}$$

Here $P^{+}_{\rm 1s}(t)$ and $P^{-}_{\rm 1s}(t)$ are the positive and negative components of the system polarization and $\hat{A}$ is a normalization coefficient. $\tilde{P}^{-}_{\rm 1s}(t',z)$ is the Laplace transform of $P^{-}_{\rm 1s}(t) = P^{-}_{\rm 1s}(t'+\tau)$ with respect to $\tau = t - t'$, where $\tau > 0$. The two-time correlation function in equation (9) are evaluated using the quantum regression theorem. To do this the density matrix elements are obtained from equation (8), assuming the IR field amplitude is slowly varying compared to the dephasing rates of the intersubband excitonic transitions. Having these in mind, we found

$$\begin{aligned}\langle[P^{+}_{\rm 1s}(\infty), \tilde{P}^{-}_{\rm 1s}(\infty,z_1)]\rangle &= |\mu^{\rm 1s}_{ij}|^2\{R^{ij,{\rm 1s}}_{8,3}(z_1)\Lambda^{ij,{\rm 1s}}_{2}(\infty) \\ &+ R^{ij,{\rm 1s}}_{8,8}(z_1)[\Lambda^{ij,{\rm 1s}}_{1}(\infty) - \Lambda^{ij,{\rm 1s}}_{7}(\infty)]\}.\end{aligned} \tag{10}$$

Here the 9×9 matrix $\mathbf{R}^{ij,{\rm 1s}}(z_1)$ is defined by

$$\mathbf{R}^{ij,{\rm 1s}}(z_1) = (z_1\mathbf{I} - \mathbf{L}^{ij,{\rm 1s}})^{-1}, \tag{11}$$

where $\mathbf{I}$ refers to the identity matrix and $\mu^{\rm 1s}_{ij}$ to the dipole moments associated with the 1s e1–hh1 to 1s e2–hh1 exciton transitions.

To find out how coherent control of $\chi^{\omega_{\rm c},I_{\rm c}}_{\rm exc}$ by the IR field influences the collective response of the MQW structure we adopt a transfer matrix method [15]. Based on this method propagation of the electromagnetic field along z through one period of the structure can be described by

$$T_{\omega_{\rm c},I_{\rm c}} = T^{1/2}_{\rm b} T_{\rm bw} T^{\omega_{\rm c},I_{\rm c}}_{\rm w} T_{\rm wb} T^{1/2}_{\rm b}. \tag{12}$$

Here the transfer matrix through one-half of the barrier is given by

$$T^{1/2}_{\rm b} = \begin{pmatrix} {\rm e}^{{\rm i}\varphi_{\rm b}/2} & 0 \\ 0 & {\rm e}^{-{\rm i}\varphi_{\rm b}/2}\end{pmatrix}, \tag{13}$$

where $\varphi_{\rm b} = \omega_{\rm s} n_{\rm b} d_{\rm b}/c$ and $d_{\rm b}$ refers to the width of the barriers. $T_{\rm bw} = T^{-1}_{\rm wb}$, which describes scattering of light by the contrast between $n_{\rm w}$ and $n_{\rm b}$, is given by

$$T_{\rm bw} = \frac{1}{1+\rho}\begin{pmatrix} 1 & \rho \\ \rho & 1\end{pmatrix}. \tag{14}$$

Here ρ is the Fresnel reflection coefficient and $T^{\omega_{\rm c},I_{\rm c}}_{\rm w}$ is the transfer matrix associated with the QW region obtained from

$$T^{\omega_{\rm c},I_{\rm c}}_{\rm w} = \begin{pmatrix} {\rm e}^{{\rm i}\varphi_{\rm w}}(1-{\rm i}S^{\omega_{\rm c},I_{\rm c}}) & -{\rm i}S^{\omega_{\rm c},I_{\rm c}} \\ {\rm i}S^{\omega_{\rm c},I_{\rm c}} & {\rm e}^{-{\rm i}\varphi_{\rm w}}(1+{\rm i}S^{\omega_{\rm c},I_{\rm c}})\end{pmatrix}. \tag{15}$$

Here $\varphi_{\rm w} = \omega_{\rm s} n_{\rm w} d_{\rm w}/c$ and $d_{\rm w}$ refers to the width of the wells. $S^{\omega_{\rm c},I_{\rm c}} = (\Gamma_0/\alpha_0)\chi^{\omega_{\rm c},I_{\rm c}}_{\rm exc}$ wherein Γ_0 is the radiative decay rate of the 1s e1–hh1 exciton and $\alpha_0 = \epsilon_\infty \omega_{\rm LT} a^3_{\rm B}\omega^2_{\rm 1s}/4c^2$. Here $\omega_{\rm LT}$ refers to the exciton longitudinal transverse splitting, $a_{\rm B}$ to the bulk Bohr exciton radius and $\omega_{\rm 1s}$ to the frequency of the 1s e1–hh1 excitons. Based on [3] for the GaAs/AlGaAs structure studied in this paper we can consider Γ_0 is around 67 μeV. Note that the MQW structure considered here is such that excitons are well localized in the wells. Additionally because of low Al content (x = 0.2), the bandgap of the barrier is direct and no implication due to the X valley states occurs.

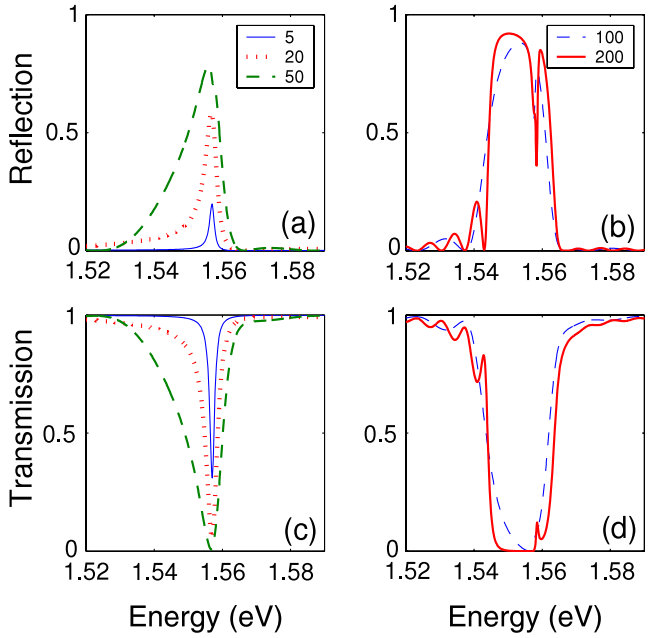

Figure 2. Reflections ((a) and (b)) and transmissions ((c) and (d)) of the MQW for different numbers of quantum well (N) in the absence of the infrared field ($I_c = 0$). Numbers in legends refer to the values of N.

3. Coherent control of multi-quantum well resonant PBG structures

To carry out the numerical calculations we assume that the well and barrier widths are 7 and 107.9 nm, respectively. In addition, one considers $n_w = 3.6$ and $n_b = 3.46$ [3]. We also consider the polarization dephasing rate associated with the non-radiative decay of e1–hh1 is 0.44 meV [16, 19] and that of e2–hh1 is 4.1 meV. Note that the former depends strongly on the quality of the sample, while the latter is mostly caused by scattering of the excitons with the optical phonons. Figure 2 shows how reflection and transmission of such a structure is changed as the number of quantum wells (N) is increased while the intensity of the control field is set to zero ($I_c = 0$). Such reflections and transmissions are the results of the enhancement of the radiative decay of e1–hh1 excitons via dominance of the superradiant mode. The sharp dip occurs around the energies of the 1s states of these excitons, which is considered to be 1.557 eV.

To study coherent control of such a PBG structure, we assume the detuning of the control field from the e1–e2 transition, Δ_c, is 5 meV and the number of the QW is 200. Reflection and transmission spectra of such a system for different values of I_c are shown in figure 3. When $I_c = 0.1$ MW cm^{-2} the amplitude of reflection is suppressed while forming a doublet (dashed line). For $I_c = 0.5$ MW cm^{-2} the lower energy peak nearly disappears and the higher energy peak becomes dominant (dashed–dotted line). The corresponding transmission spectra are also peculiar. As shown in figure 3(b), with the increase of the I_c, the photonic bandgap seems to be enhanced (dashed line). For $I_c = 0.5$ MW cm^{-2}, apparently the bandgap is enhanced further, while some features are developed within it.

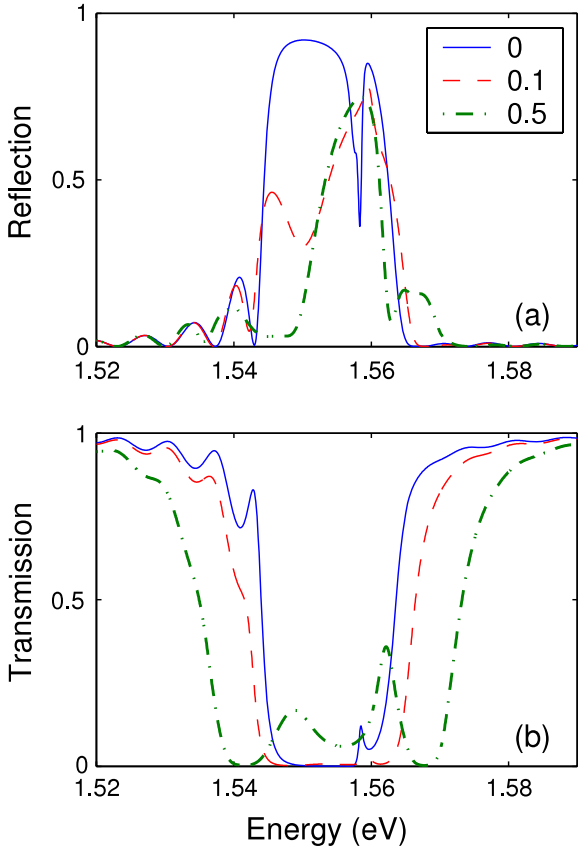

Figure 3. Variation of reflection and transmission of the Bragg MQW structure with 200 QWs for different field intensity with $\Delta_c = 5$ meV. Legends refer to the I_c in MW cm^{-2}.

Figure 4 illustrates evolution of such a system for higher control field intensities. Comparison of figures 4(a) and (c) shows that, as I_c increases further, the reflection amplitude saturates (dashed line). In other words, it becomes immune against the control field intensity. Here the reflection becomes very similar to that of an MQW with the same parameters but without any exciton effects (figure 4(c), dotted line). Removing the exciton effects allows only a non-resonant response of the system to contribute. This suggests that the transmission of the Bragg MQW system under intense infrared field reaches that of the non-resonant passive PBG structure generated by the background refractive index contrast of the wells and barriers.

The situation for the transmission is rather different. Comparing the results shown in figures 4(b) and (d) indicates that the transmission response of the MQW develops a triplet. As control field intensity increases the central peak and the two distinct sidebands become more distinct. This happens while the central peak frequency remains nearly unchanged but the sidebands are moving away from each other. It is interesting to note that the amplitude of the central peak matches that of the non-resonant response of the MQW obtained by ignoring the effects of excitons (dotted line). These results suggest that the central peak is, in fact, purely the result of background refractive index contrast of the wells and barriers and, as such, it does not change with the increase of coupling field intensity.

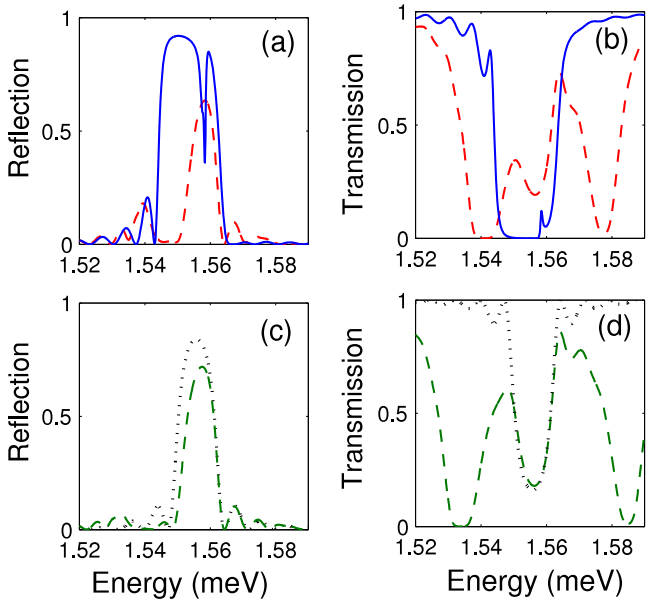

Figure 4. Similar to figure 3 but for $I_c = 1$ MW cm^{-2} (dashed lines in (a) and (b)) and for $I_c = 2$ MW cm^{-2} (dashed lines in (c) and (d)). Solid lines in (a) and (b) refer to the reflection and transmission when $I_c = 0$ and dotted lines represent the off-resonant responses of the system in the absence of the excitons.

4. Photonic bandgaps versus electromagnetically induced transparency

The results presented in figures 3 and 4 show that both reflection and transmission of the Bragg MQW structure are changing in peculiar ways under the influence of the IR laser. As will be shown in this section, these results are related to the competition between EIT generated in the single QWs (electronic coupling) and the photonic coupling generated by the combined effects of superradiant excitons and background refractive indices of wells and barriers.

To investigate this issue in more detail, we consider four different types of Bragg MQW structures. These structures are identical in all aspects except for the number of their QW periods (N). We consider $N = 20, 50, 100$ and 200, covering the range of weak to strong photonic features. Figure 5 shows the results when $I_c = 0.1$ MW cm^{-2}, i.e. low infrared coupling regime. Here we can see that for any number of QWs the reflection include two peaks, although their forms are not similar. Transmissions of such MQW structures also show more or less similar features, except for the fact that for high numbers of QW periods they are flattened, forming well-defined bandgaps (figure 5(b)).

When the intensity of the control is increased, reaching $I = 1$ MW cm^{-2}, the situation is changed dramatically. As shown in figure 6, here when $N = 20$ we can still see two peaks, one around 1.535 eV and the other around 1.57 eV, both in reflection and transmission (narrow solid lines). As the number of the QW periods increases the photonic contribution enhances. In the reflection this leads to an initial enhancement of the two peaks (dotted lines) for $N = 50$ followed by formation of a single dominant reflection peak when $N = 100$

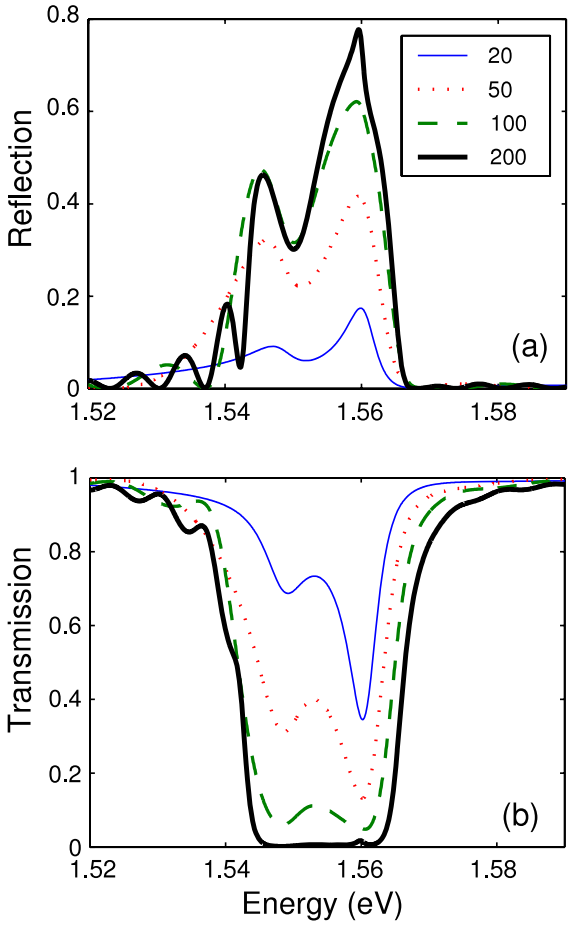

Figure 5. Variation of reflection (a) and transmission (b) of the MQW with $N = 20, 50, 100$ and 200 when $I_c = 0.1$ MW cm^{-2} and $\Delta_c = 5$ meV. The numbers in the legend refer to N.

(dashed line). For $N = 200$ the amplitude of this peak increases further. For very large N a complete PBG is formed (not shown). The transmission, on the other hand, shows a transition from a doublet for $N = 20$ to a triplet when $N = 200$.

To study these issues in more detail, let us consider how the imaginary part of the susceptibility of one period of the QW structure ($\chi_{\rm exc}^{\omega_c, I_c}$) is changed with IR field intensity. As one can see the thin solid lines in figures 5(a) and 6(a) ($N = 20$) are very similar to the dashed line in figure 7. This suggests that for small N the system is more purely electronic (excitonic). As N increases, the optical feedback becomes stronger. For small I_c (figure 6) this leads to a coherent mixture of interwell coupled excitons, i.e. both superradiant and EIT exist. On the other hand, if one considers large I_c, as figure 7 shows, excitons in individual QWs develop well-resolved doublets. The optical energy shifts associated with these doublets violate the Bragg condition that was adjusted for uncoupled exciton energies. As a result, the superradiant mode is fully destroyed and replaced by the development of the EIT mode. The EIT mode does not contribute to the reflection of the system, as it does contribute to the optical feedback of the structure (figure 6).

For the transmission the situation is rather different. As figure 6(b) shows, for small N the transmission spectra are

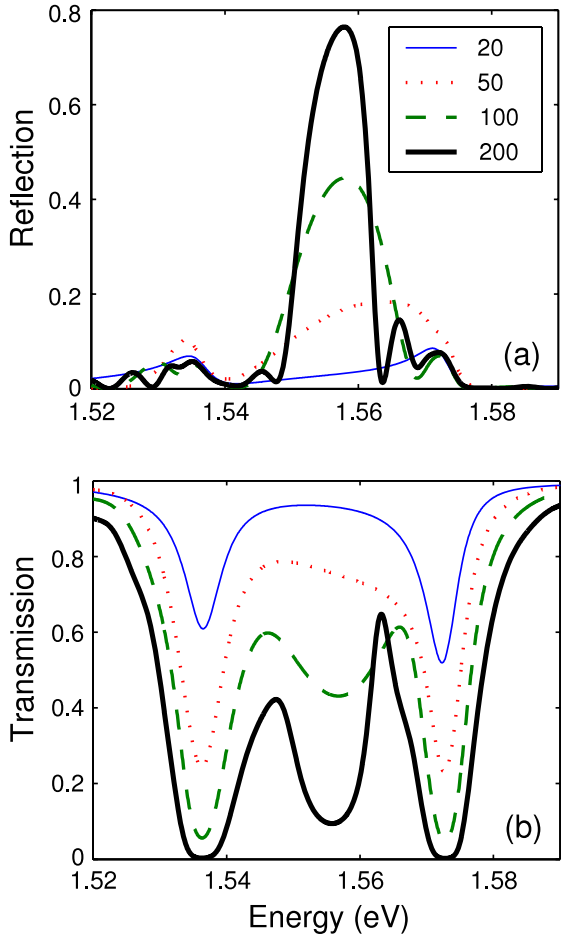

Figure 6. Similar to figure 5 but for $I_c = 0.5$ MW cm^{-2} and $\Delta_c = 5$ meV. The numbers in the legend refer to N.

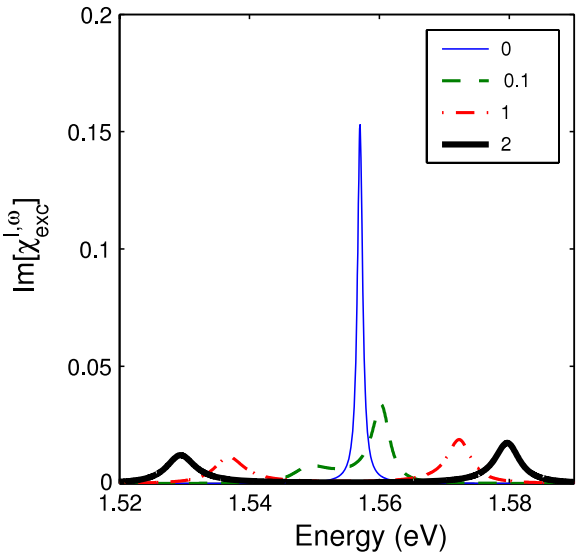

Figure 7. Variation of the imaginary part of the susceptibility with the IR field intensity. The numbers in the legend refer to I_c in MW cm^{-2}.

similar to those shown in figure 7. As N increases, however, a central peak is generated at the middle of the doublets. The fact that, for different values of I_c the sideband peaks

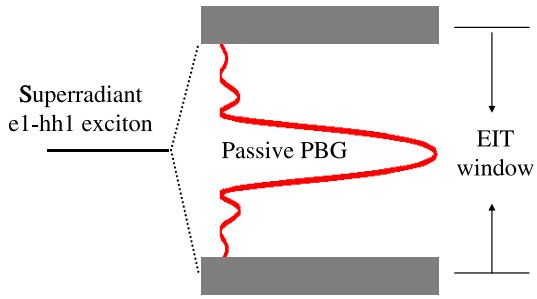

Figure 8. Schematic illustration of hybrid excitonic/photonic system. This figure shows transformation of the active PBG associated with the superradiant mode of excitons in the absence of the IR field to the hybrid photonic/electronic state.

are moving while the central peak remains unchanged, is compatible to what we see in figure 7. In other words, it indicates formation of a hybrid electronic/photonic system. The overall process of infrared switching from the active PBG to such a hybridized system is schematically summarized in figure 8. In the absence of the control field ($I_c = 0$) we have the state of the supperradiant mode. In the presence of this field with large I_c an EIT window is generated while the superradiant mode is destroyed and replaced by an EIT mode. Under this condition a transmission peak with photonic nature is superimposed at the center of the transparency window.

5. Conclusions

We studied optical control and hybridization of active PBGs via an infrared laser field. The hybridization process happened as the superradiant mode of the excitons was destroyed via their IR dressing. This study was based on manipulation of their different contributing components in Bragg MQW structures: (i) background refractive index contrast of wells and barriers, (ii) superradiant exciton or interwell coupling of the quantum wells and (iii) infrared coherent coupling of individual quantum wells. We showed that the infrared coupling allowed us to control the interplay between these three components, balancing them on demand. This led to a transition from active PBG, which was generated from the combined effects of (i) and (ii), to hybrid systems consisting of purely photonic and electronic systems. These results hold the promise of novel optical material systems, ultra-fast all-optical switches and new development in coherently controlled optical processes in semiconductors.

References

[1] Evchenko E L, Nesvizhskii A I and Jorda S 1994 *Phys. Solid State* **36** 1156
[2] Hubner M, Prineas J P, Ell C, Brick P, Lee E S, Khitrova G, Gibbs H M and Koch S W 1999 *Phys. Rev. Lett.* **83** 2841
[3] Hubner M, Kuhl J, Stroucken T, Knorr A, Koch S W, Hey R and Ploog K 1996 *Phys. Rev. Lett.* **76** 4199
[4] Sadeghi S M, Li W, Li X and Huang W-P 2006 *Phys. Rev.* B **74** 161304(R)
[5] Scully M O and Zubiary M S 1997 *Quantum Optics* (Cambridge: Cambridge University Press)

[6] Serapiglia G B, Paspalakis E, Sirtori C, Vodopyanov K L and Phillips C C 2000 *Phys. Rev. Lett.* **84** 1019
[7] Sadeghi S M and Li W 2005 *IEEE J. Quantum Electron.* **41** 1227
[8] Singh M R 2004 *Phys. Rev.* A **70** 033813
[9] Artoni M and Rocca G C L 2006 *Phys. Rev. Lett.* **96** 073905
[10] Johnston W J, Yildirim M, Prineas J P, Smirl A L, Gibbs H M and Khitrova G 2005 *Appl. Phys. Lett.* **87** 101113
[11] Prineas J P, Zhou J Y, Kuhl J, Gibbs H M, Khitrova G, Koch S W and Knorr A 2002 *Appl. Phys. Lett.* **81** 4332
[12] Prineas J P, Johnston W J, Yildirim M, Zhao J and Smirl A L 2006 *Appl. Phys. Lett.* **89** 241106
[13] Yang Z S, Kwong N H, Binder R and Smirl A L 2005 *J. Opt. Soc. Am.* B **33** 2144
[14] Yang Z S, Kwong N H, Binder R and Smirl A L 2005 *Opt. Lett.* **30** 2790
[15] Erementchouk M V, Deych L I and Lisyansky A A 2005 *Phys. Rev.* B **71** 235335
[16] Deych L I, Erementchouk M V and Lisyansky A A 2004 *Phys. Rev.* B **69** 075308
[17] Zhu B 1988 *Phys. Rev.* B **37** 4689
[18] Sadeghi S M and Li W 2005 *Phys. Rev.* B **72** 075347
[19] Prineas J P, Ell C, Lee E S, Khitrova G, Gibbs H M and Koch S W 2000 *Phys. Rev.* B **61** 13862